Camera-based spatter detection in laser welding with a deep learning approach

Julia Hartung[1,2], Andreas Jahn[1], Martin Stambke[1], Oliver Wehner[1], Rainer Thieringer[1], and Michael Heizmann[2]

[1] TRUMPF Laser GmbH,
Aichhalder Straße 39, 78713 Schramberg
[2] Karlsruher Institut für Technologie,
Institut für Industrielle Informationstechnik,
Hertzstraße 16, 76187 Karlsruhe

Abstract Continuous quality monitoring is essential for automated production systems and efficient manufacturing. Laser welding processes are a key technology for many industrial applications and must fulfill high-quality requirements. Various influencing factors can lead to defects in the weld seam, which impair the functionality and quality of the end product. Therefore, a reliable quality assurance is a prerequisite for high product quality in welding processes. An indicator for an unstable situation in welding processes is the occurrence of spatter on the component. Thus, the detection of spatter can serve as a significant signal for defective weld seams. This article proposes the detection of spatter based on a camera image taken with an industrial camera, which is usually already integrated in the laser system. Due to the large variance of weld seams in image-based analysis, algorithms with a high degree of generalization are required. Using convolutional neural networks (CNN) and semantic segmentation the camera image is analyzed and classified pixel by pixel. The CNN is trained in a multi-class approach in order to recognize the weld seam as well as the spatter as result classes. The segmentation map constitutes the classification result. The results of the deep learning algorithms are evaluated by different methods and conclusions about their prediction quality are made.

Keywords Laser welding, semantic segmentation, u-net, quality assurance, spatter detection

DOI: 10.58895/ksp/1000124383-25 erschienen in:

Forum Bildverarbeitung 2020

DOI: 10.5445/KSP/1000124383 | https://www.ksp.kit.edu/site/books/m/10.58895/ksp/1000124383/

1 Introduction

Laser welding is a key technology in many industrial applications. Due to various advantages, like the possibility to create narrow but deep welding seams and the contactless assembly at highest processing speed, the procedure is more and more used in industry [1, 2]. Remote-controlled laser welding with scanner optics can be integrated as process step in an automated production system and is thus becoming increasingly relevant [3]. To ensure a high welding quality, continuous process monitoring is essential [3, 4].

Various influencing factors can lead to defects in the weld seam, which impair the quality and functionality of the end product and often result in safety-relevant risks. In the context of quality assurance, the presence of spatter on the component can be used as an indicator of an unstable situation in the welding process, as its occurrence is closely related to the quality of the weld seam [5, 6]. Spattering is the ejection of melt droplets from a molten bath [4]. There are different types of spatter phenomena that can occur during laser welding. In [7] the formation of spatter and different types of spatter was investigated and a system for categorizing spatter formation was proposed. The effects of droplet ejection from the weld metal can result in a weld seam with underfill, undercuts, craters, blowholes or eruptions that can negatively affect weld properties [7]. Spatter detection therefore serves as a significant signal for defective welds.

As spatters represent height deposits, they can be easily and clearly detected by means of optical coherence tomography (OCT) (figure 3.1a and 3.2a). Just simple image processing algorithms applied on the depth maps such as threshold analysis are necessary. Even if the evaluation of the sensor data is simple and unambiguous, the use of the sensor in this application case has disadvantages. In order to use the OCT sensor, it must first be installed and set up explicitly for quality monitoring on the system. The sensor, which is already expensive to purchase, generates additional effort through calibration procedures and increases the complexity and cost of the overall construction of the system and optics.

By observing the welding process in real time, spatter can be detected as it occurs. In [8], for example, the welding process is monitored by an external high-speed video camera which is sensitive in

the ultraviolet and visible wave length range and captures dynamic images of laser welding plume and spatter directly during the welding. The number and size of the spatters were calculated by using image processing technology and defined as characteristic features. Furthermore, the use of an external high-speed camera for near infrared (IR) measurements was tested. A direct comparison of the images showed, however, that the measurement in UV light and visible light was more suitable for spatter detection [4].

In [9] a setup with a CMOS camera directly at the laser optics is proposed for monitoring the welding process. To get significant images of the weld pool an additional laser for confocal illumination is used and a bandpass filter is placed in front of the camera. Based on the generated images, approaches for scanning the contour of the melt lake and an approach for spatter detection using outlier classification were presented [9].

In comparison to the system setup of the approaches introduced above, an industrial camera is usually already integrated in the system. The camera image is used for example to detect the position of components before welding. However, it is difficult to analyze the weld seams based on images using conventional image processing methods. Even faultless welding seams show a high variance, so that the image processing algorithm for spatter detection must be adapted by experts for each welding process.

Compared to conventional image processing algorithms, deep learning methods tolerate natural deviations in complex patterns. Convolutional neural networks (CNN) offer the advantage that they can be adapted to new procedures without expert knowledge by training procedures, which has already led to very good results. For example in [10] an auto-encoder is used to learn relevant features from the input data. They use a deep neural network to extract salient and low-dimensional features from the high-dimensional laser welding data.

This article proposes the detection of spatter directly after the welding process using the camera image, which does not contain any information about the height profile. Due to the large variance of weld seams in image-based analysis, algorithms with a high degree of generalization are required. The experimental setup is described in section 2 , which is split into the generation and explanation of the

data basis, as well as the analysis and classification of the camera image. In section 2.1, the structure of the neural network is described in more detail and in 2.2 the evaluation methods are further specified. The results are discussed in section 3. A conclusion with a summary of the described algorithms is given in section 4.

2 Experimental setup

The data analysis is performed on 18 mm long weld seams, which connect two sheets with each other. For this study we carried out welding experiments on different materials and with different configurations. The occurrence of spatter as well as the quality of the weld seam depends strongly on the welding parameters. During the experiment we varied the laser power between 4 kW and 6 kW, created a gap between the sheets and induced a defocusing of the scanner optics. This influenced the process in such a way that spatter and also unstable weld seams were produced.

Immediately after welding we took a grayscale camera image with an industrial camera and scanned the height profile of the seam area with an OCT sensor. Both sensors are mounted directly on the welding head and run coaxially with the laser beam path through the beam focusing optics. To get a better camera view, a lighting ring is attached to the scanner optic. By recording both camera and OCT data on a weld seam, the reliable information about the occurrence of spatters can be derived from the height information and used as ground truth. This enables an evaluation of the accuracy of the camera-based prediction, even in cases where the spatters may not be intuitively visible in the camera image.

2.1 Network architecture

A semantic segmentation approach was chosen to evaluate the seam and to recognize spatters in the camera image. The architecture of the convolutional network is based on the u-net architecture [11]. The network learns the structure of the weld seam and the properties of the spatter class in the convolution layers and can thus perform a correct assignment of the image areas. The u-net architecture

relies on the strong use of data augmentation. Data augmentation is essential to teach the network the desired invariance and robustness properties for training with only a few training data sets [11]. Since labeling in semantic segmentation is time-consuming and error prone, it is useful to work with a small amount of training datasets especially in industrial applications. The previously generated data set is enlarged by rotation, vertical and horizontal shift, vertical and horizontal flip, adjustment of the brightness range, zoom and shear, which also improves the robustness of the training. In general, the images were only cut to the seam area during pre-processing and left in their original condition for better performance. Four different classes were defined as output. One class covers the background, another the weld seams welded with optimal parameters, the third class unstable weld seams and the fourth class the spatters.

The network architecture has been reduced in size compared to the original u-net. It is recommended to keep the number of trainable parameters in the architecture low, especially since industrial process images have less variability and less complex properties. In the downsampling the network architecture contains six convolutional layers and three max-pooling layers that each reduce the resolution by a factor of two. Each convolutional layer is followed by an exponential linear unit (ELU), which increases the convergence rate during learning. The ELU was proposed by Clevert et al. [12] as a self-normalizing layer that extends and improves the commonly used ReLU activation. It helps to prevent the Dying-ReLU problem, since it's derivative is different from zero for negative values. Several other studies have shown improvements in training and results as well. Our tests confirm these results, which is why we use the ELU function in the network architecture. The number of feature channels is doubled per downsampling step similar to the original u-net architecture. After the corresponding upsampling a final layer with a 1x1 convolution followed by a softmax activation is used to map each feature vector to the desired number of classes.

The model is not pretrained, but the Xavier Glorot uniform initialization method is used to initialize the weights [13].

2.2 Evaluation

Training approaches with two different loss functions were evaluated. The first approach uses the weighted categorical cross entropy loss (WCCE) and the other the weighted dice coefficient loss function.

Since the number of pixels per class is very different and especially the less important background class contains most pixels, the weighting in the loss function generates better results. The pixel ratio values of the different classes are as follows: background: 82%, seam welded with optimal parameter: 6.3%, unstable weld seam: 11.6% and spatter 0.1%. In comparison, the frequency of occurrence of the classes in all images is follows: background: 100%, stable weld seam: 33.3%, unstable weld seam: 66.6% and spatters 86%.

The class weight has been defined to give priority to the evaluation of the weld seam and also to force the detection of spatter. We choose a weighting of 0.1 for the background, 0.25 each for stable weld seam and unstable weld seam and 0.4 for the spatter class. Attention must be paid to ensure that the weighting does not penalize the most common class (background) too much, otherwise some pixels will no longer be classified. Therefore a good ratio for the weightings must be found.

The neural network was trained with a training data set of 251 images. 74 images are of weld seams welded with optimal parameters, while the other 177 images show weld seams that establish the different defect classes. For labeling the camera images depth data on basis of the OCT data are used as ground truth. With the knowledge of the height information all spatters can be recognized and labeled. The weld seams and spatters were marked (optimally welded seams in green, defective weld seams in blue and spatters in red, see figure 3.1c and figure 3.2c). With a good setting of the laser parameters, far fewer spatters are produced than with poorly selected parameters. Therefore, spatter occurs more often with defective welds than with good ones.

A quarter of the training data was used as validation data set.

3 Results

After training of 184 epochs with 150 steps per epoch, a batch size of 20 and the use of the weighted dice coefficient loss function a training error of 0.13 and validation error of 0.23 was achieved. The weighted dice coefficient loss function provides better results than the WCCE approach.

To evaluate the result the weighted dice coefficient loss, also known as the Sørensen-dice coefficient or F1 score, is used too. Therefore, we use the function

$$\text{Loss function} = 1 - \text{dice} \tag{3.1}$$

with

$$\text{dice} = \frac{2 \mid X \cap Y \mid}{\mid X \mid + \mid Y \mid} \tag{3.2}$$

where $\mid X \mid$ and $\mid Y \mid$ are the cardinalities of the two sets.

The dice value is calculated for each individual class, weighted with the respective class weighting and then added up.

The loss value on the test data set is 0.27. If only the spatter class is taken into account, a loss value of 0.32 is achieved. It must be considered that the spatters contain only very few pixels compared to the total image and that these cannot always be labeled exactly on basis of the ground truth.

Figure 3.1 and figure 3.2 show examples of segmentation maps predicted by the neural network trained with the weighted dice coefficient loss function. In both examples the spatters were detected, and the welding seam was correctly classified as being welded with optimal parameters or as a weld of poorer quality. In figure 3.1(a) the weld seam and three spatters are shown in an image generated from the height profile of the OCT sensor. In figure 3.1(b) the corresponding camera image of the same weld with spatter is shown. The grayscale image is analyzed using a deep learning approach and classified with pixel-level semantic segmentation according to weld seam and spatter. The result is shown in figure 3.1(c). The detected

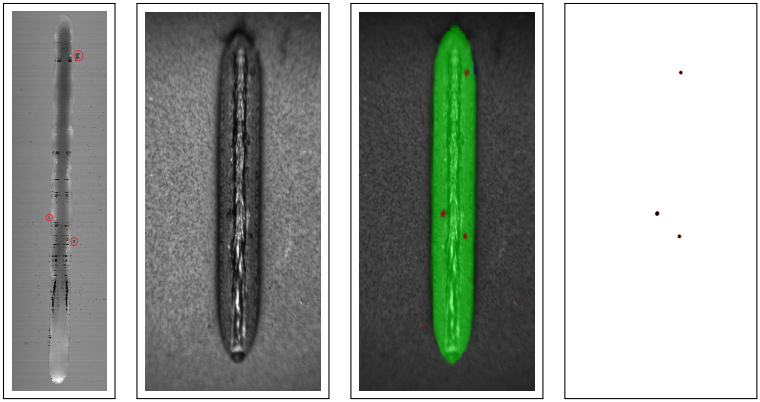

Figure 3.1: (a) image generated on the depth data on basis of the OCT sensor, (b) camera image, (c) overlay image with the predicted segmentation map, (d) detected spatters

seam is labeled in green, while the spatters are labeled in red. Figure 3.1(d) shows the detected spatters counted for the comparison with the ground truth. Corresponding to figure 3.1 the different pictures of an error seam are shown in 3.2. In this case the detected seam is labeled in blue, because it is a weld seam of poor quality.

However a better comparison is provided by the number of detected spatters in the image compared with the number of spatters in the ground truth. In this evaluation approach the precisely labeled pixels are not important, only the amount of detected spatters is taken into account. With a test data set of 102 images, an average deviation of 0.41 spatters per image was observed. The number of spatters was correctly detected in 77 of the images. In the other cases either not all spatters were detected or discoloration in the sheet or on the welding seam was also classified as spatter. The ratio between the two error cases is quite balanced. The highest deviations were caused by the test sets containing many spatters. With 5 misclassifications, these are very significant in the average result value. In figure 3.3 the classification result of the test data set is shown in a more detailed way. The number of spatter in the ground truth is

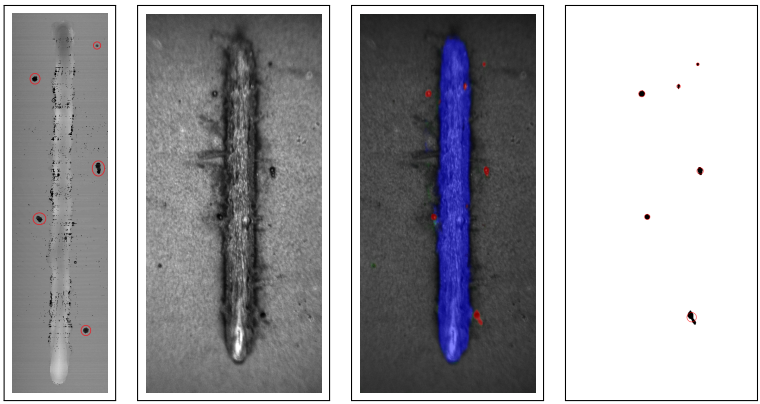

Figure 3.2: (a) image generated on the depth data on basis of the OCT sensor, (b) camera image, (c) overlay image with the predicted segmentation map, (d) detected spatters

compared to the number of spatter in the prediction. The two cases in which 5 spatter were not detected are shown in the bottom two lines at ground truth 10 and 11. But more decisive for the weld seam evaluation are the cases in which a picture is classified as spatter-free despite spatter in the ground truth, or the other way round in which spatters are detected in a picture that has no spatter in the ground truth. These cases would lead to false conclusions about the seam quality and should therefore be avoided. In our test data set spatters were classified on two images although there were none in the ground truth and once no spatter was found on the test image although the ground truth indicated two small spatters. These values are shown in figure 3.3 at ground truth 0 and prediction 1 and the other case at ground truth 2 and prediction 0.

In our Test dataset of the 102 test images, too few spatters were detected on 13 images and too many spatters on 12 images.

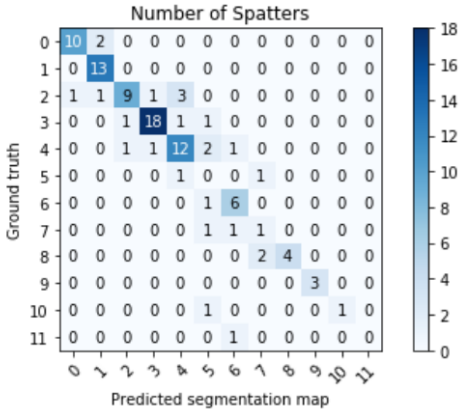

Figure 3.3: Comparison of the number of spatter in the ground truth and the prediction in the test data set

4 Conclusion

In this paper an approach for spatter detection in a laser welding process with an industrial camera was presented. This was achieved by using a semantic segmentation approach to slim down the image features and classify the image pixel by pixel. Even with a small training data set all spatters could be correctly classified on 75% of the images from the test data set. Only on 3 out of 102 test images no spatter was detected in spite of existing spatters in the ground truth, or spatter was detected on images that actually contained no spatter. This results in an effective error rate with wrong conclusion of 2.9%. This result proves that quality monitoring is possible with a simple system setup. The setup of a fixed industrial camera is mostly standard in laser welding due to seam position control or other functions required for welding. This means that process monitoring can be done without additional hardware and the resulting costs or installation work. This aspect should not be ignored when implementing a system in industry. In addition, neither high-resolution images nor complex pre-processing algorithms were used, which would require longer processing time and higher computing power. Promising results were achieved on the industrial data set,

which justifies an image-based quality assessment using deep learning in the industrial environment.

References

1. M. Jäger, S. Humbert, and F. Hamprecht, "Sputter Tracking for the Automatic Monitoring of Industrial Laser-Welding Processes," *IEEE Transactions on Industrial Electronics*, vol. 55, pp. 2177–2184, 2008.
2. A. Bollig, S. Mann, R. Beck, and S. Kaierle, "Einsatz optischer Technologien zur Regelung des Laserstrahlschweißprozesses," in *Autom.*, 2005.
3. M. Zaeh, J. Moesl, J. Musiol, and F. Oefele, "Material processing with remote technology revolution or evolution?" *Physics Procedia*, vol. 5, pp. 19 – 33, 2010, laser Assisted Net Shape Engineering 6, Proceedings of the LANE 2010, Part 1.
4. D. You, X. Gao, and S. Katayama, "Visual-based spatter detection during high-power disk laser welding," *Optics and Lasers in Engineering*, vol. 54, pp. 1 – 7, 2014.
5. A. Kaplan and J. H. Powell, "Laser welding: The spatter map," *International Congress on Apllications of Laser & Electro-Optics*, pp. 683–690, 2010.
6. M. Zhang, G. Chen, Y. Zhou, S. Li, and H. Deng, "Observation of spatter formation mechanisms in high-power fiber laser welding of thick plate," *Applied Surface Science*, vol. 280, pp. 868 – 875, 2013.
7. A. Kaplan and J. H. Powell, "Spatter in laser welding," *Journal of Laser Applications*, vol. 23, pp. 1–7, 2011.
8. X. Gao, Y. Sun, and S. Katayama, "Neural network of plume and spatter for monitoring high-power disk laser welding," *International Journal of Precision Engineering and Manufacturing-Green Technology*, vol. 1, pp. 293 – 298, 2014.
9. N. C. Stache, H. Zimmer, J. Gedicke, A. Olowinsky, and T. Aach, "Robust High-Speed Melt Pool Measurements for Laser Welding with Sputter Detection Capability," in *DAGM07: 29th Annual Symposium of the German Association for Pattern Recognition*, ser. LNCS, F. A. Hamprecht, C. Schnörr, and B. Jähne, Eds., vol. 4713. Heidelberg: Springer, Sept. 12–14 2007, pp. 476–485.
10. J. Günther, P. M. Pilarski, G. Helfrich, H. Shen, and K. Diepold, "Intelligent laser welding through representation, prediction, and control learning: An architecture with deep neural networks and reinforcement

learning," *Mechatronics*, vol. 34, pp. 1 – 11, 2016, system-Integrated Intelligence: New Challenges for Product and Production Engineering.

11. O. Ronneberger, P. Fischer, and T. Brox, "U-Net: Convolutional Networks for Biomedical Image Segmentation," *CoRR*, vol. abs/1505.04597, 2015.
12. D.-A. Clevert, T. Unterthiner, and S. Hochreiter, "Fast and Accurate Deep Network Learning by Exponential Linear Units (ELUs)," *CoRR*, vol. abs/1511.07289, 2016.
13. X. Glorot and Y. Bengio, "Understanding the difficulty of training deep feedforward neural networks," in *AISTATS*, 2010.